Capacitance performance of NiO thin films synthesized by direct and pulse potentiostatic methods

Yasser Ghalmi[a], Farid Habelhames[a*], Abdelfetteh Sayah[a], Ahmed Bahloul[a], Belkacem Nessark[a], Manal Shalabi[b], Jean Michel Nunzi[b]

[a] Laboratoire d'Electrochimie et Matériaux (LEM), Faculté de Technologie. Département de Génie des Procédés, Université Ferhat Abbas Sétif 1, 19000, Algérie

[b] Department of Chemistry, Queen's University, Kingston, ON K7L 3N6, Canada
* Corresponding Author

Abstract

Transition metal oxides have applications into energy storage devices such as electrochemical supercapacitors. We deposited nickel oxide (NiO) thin films using electrodeposition under direct and pulse potentiometry. Effects of the pulse electrodeposition conditions are systematically investigated. Results show that the pulse time clearly influences the morphology of the deposited thin films. The nanostructured thin film that was deposited under 1 sec on-time condition proved to be a suitable electrode material since its 1000 Fg^{-1} at 0.5 Ag^{-1} specific capacitance is large enough to fulfil the needed requirement. In addition, the thin film at hand shows 90.1% capacity retention during 800 galvanostatic charge–discharge cycles under 5 Ag^{-1} current density. Moreover, nanostructured NiO films prepared by pulse electrodeposition demonstrate high power performance, excellent rate as well as long term cycling stability, which make them promising electrode materials for supercapacitor applications.

Keywords: NiO; Thin film; Electrodeposition; Supercapacitor; Chronopotentiometry; Pulse potentiometry.

1. Introduction

Owing to their remarkable technical features, supercapacitors embody what is known nowadays as next generation energy storage, which is required in many technological sectors including power supply devices. The important role of supercapacitors in power source applications is not only due to their ability to supply short-term power to mobile electronic devices, but also to supply auxiliary power for hybrid electric vehicles similar devices [1-6]. Thus, batteries and fuel cells are being more and more overcome and replaced by electrochemical supercapacitors (Ecs) as smart energy storage devices in high energy density and power applications [7-13].

Based of charge storage mechanisms, Ecs are divided into two primary categories: electrical double layer capacitors (EDLCs) and pseudocapacitors. The former i.e. EDLCs store charge electrostatically through adsorption at the electrode/electrolyte interface by means of the large surface areas conductive electrodes [2]. Pseudocapacitors store charges following simultaneous faradic reactions at the electrode surface and within the bulk. As a result, pseudocapacitors have higher specific capacitance (SC) than EDLCs [9,14]. Structure of the electrode materials plays an important role in the determination of the electrolyte accessibility and stability in pseudocapacitors [15]. Thus, textured porous electrode materials with large surface area are preferred [16]. Porous nanostructures can be synthesized by cathodic electrodeposition [7,17].

Research on transition metal oxides as electrode materials for supercapacitors is still under way [18-21]. Nickel oxide (NiO) for instance is one valuable alternative due to its activity as electrode materials, large theoretical specific capacitance, low cost and low environmental impact [22]. However, it also suffers low electrical conductivity that may generate high internal resistance and poor performance in electrochemical devices [23].

The importance and complexity of the issue requires elaborated and well adapted methods to improve the electrical conductivity of the metal oxide electrodes. Electrochemical deposition synthesis is much simpler and economical [24-28] than conventional elaboration like molecular beam epitaxy [30], cathodic sputtering [31], laser ablation [32] or chemical vapor deposition [33]. Among the electrodeposition operational factors (temperature, electrolyte concentration), the most effective one in controlling composition and properties of the coatings is the pulse current (PC). Compared to direct current (DC), PC has proved to be an interesting alternative for improving/modifying coating quality [34,35]. In the pulse current method, the operational variables under control are peak current density (I_p), average current density (I_a), on-time (t_{on}), off-time (t_{off}), pulse frequency (f) and duty cycle (θ). The peak current is the current during on-time. The duty cycle in the 1–100% range is calculated according to Eq. (1)

$$\theta = (t_{on}/(t_{on}+t_{off})) * 100 \quad (1)$$

Frequency is given by Eq (2):

$$f = 1/(t_{on}+t_{off}) \quad (2)$$

Whereas in DC electrodeposition the current density (D_k) is the sole free parameter, in PC technique I_p, t_{on} and t_{off} can be adjusted independently. Subsequent changes in charge and mass transfer affect the morphology, chemical composition and properties of the coating.

In this work, we investigated the thin film deposition upon imposing deposition time t_{on} through pulse electrodeposition, compared to direct electrodeposition in a nickel sulphanate bath without additives to minimize contamination sources. Processing parameters were then modified in order to refine the NiO nanoparticles morphology. The elaboration was carried out through chronoamperometry in continuous and pulse

regimes. Coatings were characterized by microstructural analysis: SEM, DRX and MET. Supercapacitive performance of the prepared NiO was evaluated by cyclic voltammetry (CV) and galvanostatic charge–discharge (GCD) tests, confirming its potential as supercapacity.

2. Experimental

All products used in this work were analytical reagent grade and used without further purification. FTO/NiO films were prepared electrochemically from a solution of 0.1M $NiSO_4$ (Sigma-Aldrich), 0.1M Na_2SO_4 (Sigma-Aldrich) and 0.1M CH_3COONa (Sigma-Aldrich) in deionized water at 65 °C with pH=5.5 by applying a constant cathodic potential of 0.91 V vs SCE using both methods: direct electrodeposition (DE) and pulse electrodeposition (PE). The NiO deposition processes was carried by DE, PE (t_{on}=1s) and PE (t_{on}=3s) to obtain three different samples labelled as N1, N2, and N3 respectively.

Direct electrodeposition is achieved by chronoamperometry in which the working electrode potential is stepped at 0.91 V vs SCE for 900 s and the resulting faradic current is monitored as a function of time [26,36-38]. Nickel oxide pulse electrodeposition is carried out potentiostatically using different cathodic square wave pulses with complete current cut-off in between pulses [15,35]. Optimized pulse plating parameters lead to acceptable deposition as shown in Table 1.

Table 1: Pulse electrodeposition parameters.

Parameter	t_{on}	t_{off}	E_{on} (V/SCE)	E_{off} (V/SCE)	Cycle number	Frequency (*f*)	Duty cycle (θ)
FTO/NiO-(N2)	1s	100ms	0.91	0.13	900	0.90	90.90
FTO/NiO-(N3)	3s	100ms	0.91	0.13	300	0.32	96.77

Electrodeposition was carried in the presence of water. H_2O can be electrochemically reduced, which can lead to nickel hydroxide and oxide formation [24,26].

$$2H_2O + 2e^- \leftrightarrows 2OH^- + H_2 \quad (3)$$

The reaction mechanism proposed in the literature for anodic electrodeposition is [39]:

$$Ni^{2+} \xrightarrow{-e^-} Ni^{3+} \xrightarrow{OH^-} NiOOH \underset{}{\overset{e^-}{\rightleftharpoons}} Ni(OH)_2 \quad (4)$$

Hydroxide films were heated till 100°C for 10 min to yield NiO. The Ni^{2+} ions originating from nickel sulphate dissolve into the deposition bath. They undergo oxidation following the application of an anode potential or current to transform into Ni^{3+} ions, which come into contact with the OH^- aqueous medium to give nickel oxyhydroxide (NiOOH). Nickel oxide is obtained following heat treatment:

$$Ni(OH)_2 \xrightarrow{kT} NiO + H_2O \quad (5)$$

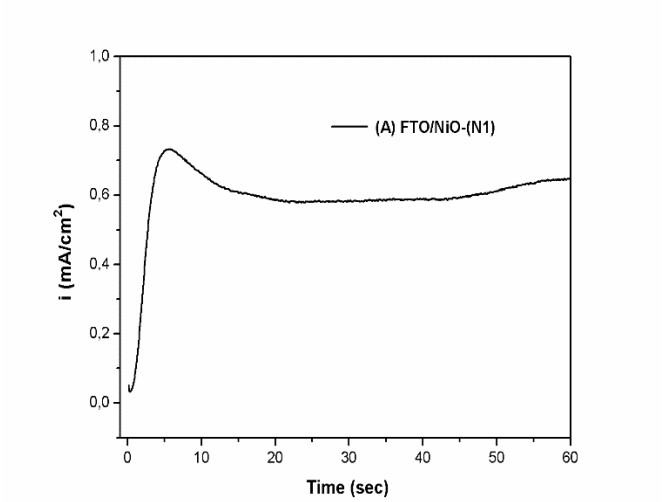

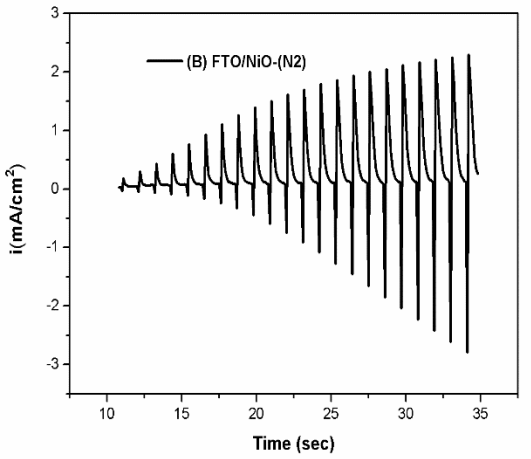

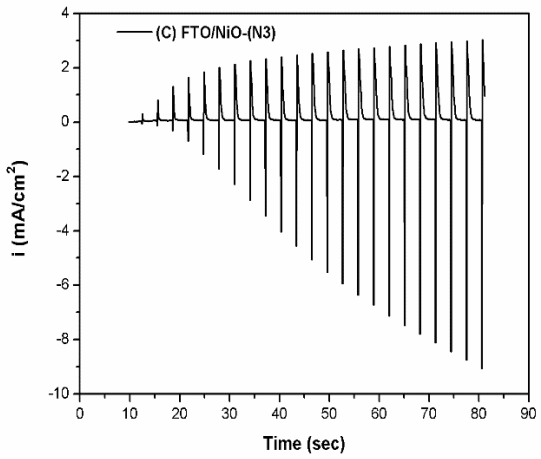

Figure 1. (A) FTO/NiO-(N1) chronoamperogram (direct current), (B) FTO/NiO-(N2) and (C) FTO/NiO-(N3) pulse electrodeposition.

Electrochemical tests were carried out at normal environment temperature inside a single compartment cell using a PGZ-301 Voltalab potentiostat connected to a computer with voltamaster 4 operating software. The latter enables control of the aimed electrochemical parameters. Electrochemical measurements were operated in a three-electrode cell using fluorine doped tin oxide glass substrate (FTO) as working electrode, a saturated calomel electrode (SCE) as a reference and a graphite rod as the auxiliary electrode.

NiO films were examined by different methods. X-ray analysis was carried out with a Rigaku model RINT 2100 powder X-ray diffractometer with a 1.54 Å CuKα-

source. Micrographs were taken from a Neo Scope JEOL JCM-5000 scanning electron microscope (SEM). Transmission electron microscopy (TEM) images were taken from a Hitachi H-7000 operated at 75 kV-accelerating voltage.

3. Results and discussions:

Figure 2 shows the XRD patterns of NiO thin films grown by DE and PE at different t_{on}. X-ray spectra are presented after subtraction of the JCPDS 00-001-0657 FTO conductive glass peaks. Results show peaks at 2θ = 37°, 43° and 62°. Peaks values nearly resemble the cubic NiO, which is in very good agreement with the standard JCPDS 01-073-1519 values [36, 37]. It can be seen that crystallinity and preferential orientation depend on the deposition time. The (200) thin film diffraction intensity increases with t_{on} -decrease.

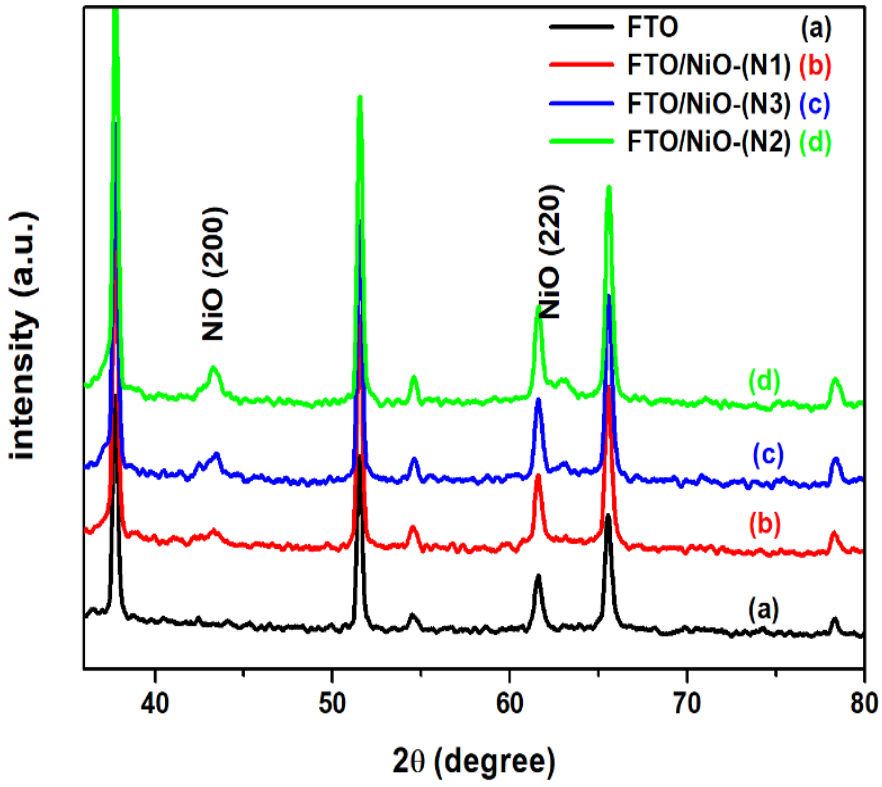

Figure2. XRD spectra of (a) FTO, (b) FTO/NiO-(N1), (c) FTO/NiO-(N3) and (d) FTO/NiO-(N2).

Morphology of the different products was examined by scanning electron microscopy (SEM) and transmission electron microscopy (TEM). Figure 3 shows the surface morphology of nickel oxide films deposited in the DE and PE modes. The nickel oxide films show a significantly different surface morphology depending on the parameters used. They exhibit a compact and quite homogeneous surface morphology. t_{on} increase to 1s changes the film surface morphology to a porous texture with nanoscale pore size leading to large cavities.

Such morphology may result in large surface area for the electrode/electrolyte interface [15,25,26], large volume/space for the active electrode material and shortened path for electrolyte penetration. These characteristics might enhance electrolyte diffusion and wettability of the electrode material for enhanced super-capacitive performances.

Wu et al. [40] used nickel sulphate as a nickel precursor to anodically deposit NiOOH at two different potentials 0.9 V / Ag / AgCl and 1.05 V / Ag / AgCl. The resulting porous morphology consisted into interconnected nanopoints. Pore size depended on the applied potential during electrodeposition, the lower the potential, the larger the pores.

TEM images illustrate the formation of NiO nanowires as synthesised under high-frequency pulse mode as compared to DE synthesised NiO material. These nanowires insure a contact between NiO grains.

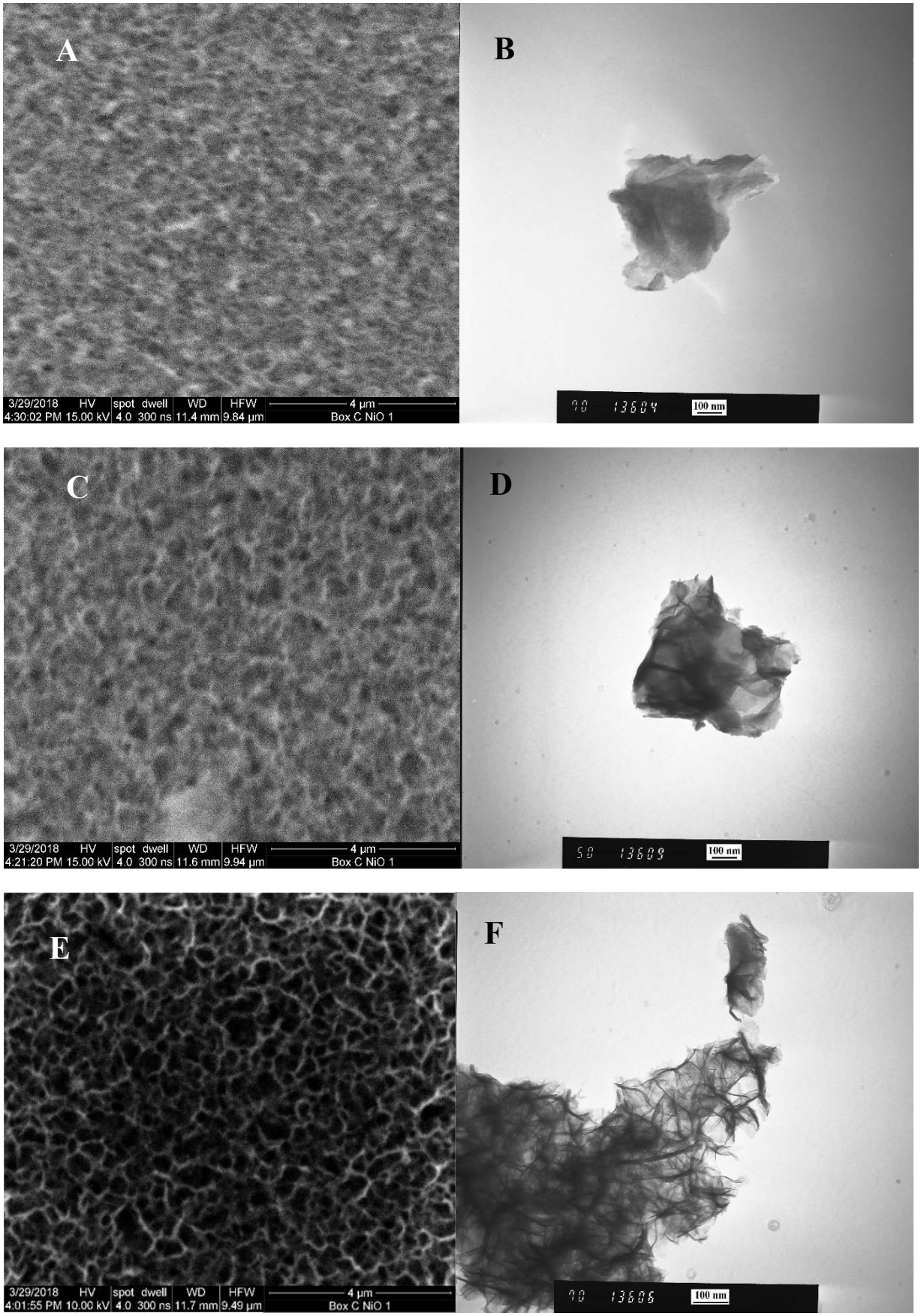

Figure 3 FTO/NiO SEM (left) and TEM (right) images: (A, B)-N1, (C, D)-N3 and (E, F)-N2.

FT-IR analysis of the synthesized samples helps understand the composition of the products. Figure 4 shows the FT-IR transmission spectra of the samples of NiO (N1, N2 and N3). Metal oxides such as NiO generally give absorption bands below 800 cm^{-1} arising from inter-atomic vibrations [41,42]. The peak at 520 cm^{-1} shows Ni–O stretching vibration and is clear evidence of the presence of the crystalline NiO [43,44]. The band at approximately 3460 is due to the (O–H) stretching vibration of the adsorbed water. The peak at about 1054 cm^{-1} in both samples is attributed to the carbonate groups, which originate from the reaction of the samples with CO_2 from air during the analysis procedure.

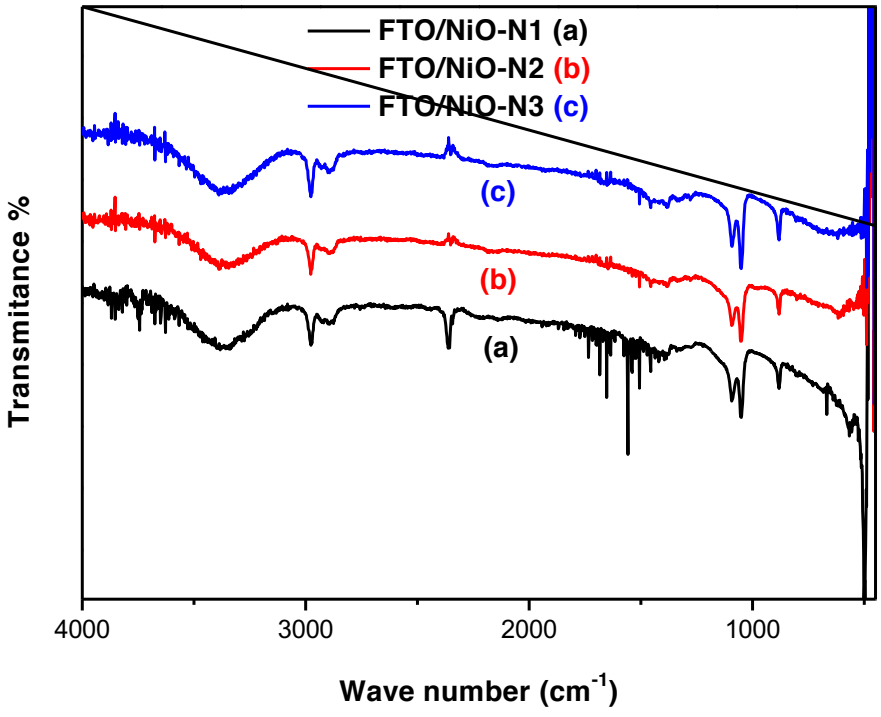

Figure 4. FTIR spectrum of the samples of NiO (N1, N2 and N3).

The electrochemical performance of NiO films was tested by cyclic voltammetry in a three-electrode configuration using 1M KOH [45] in the potential range 0 to 0.55 V vs. SCE at different scan rates: 5, 10, 20, 30, 50 mVs^{-1}.

Cyclic voltammograms of the deposited nickel oxide films at different scan rates are shown in Figure 5. All samples show a typical redox peaks pair, suggesting a battery-type electrochemical behaviour. It is attributed to the faradaic redox reaction of NiO/NiOOH [24,37] as follows:

$$NiO + OH^{-} \leftrightarrow NiOOH + e^{-} \quad (6)$$

FTO/NiO-(N2) shows the largest enclosed CV area and the highest peak current among pristine NiO and other samples, demonstrating the largest charge-storage capacity. We see that increasing the PE mode frequency increases the specific capacity of NiO samples as compared with the DC mode. The linear relationship between $v^{1/2}$ and the cathodic peak current of NiO films indicates the good reversibility and the presence of diffusion-controlled reactions in NiO. In other words, NiO behaves as pseudocapacitive or battery-like material.

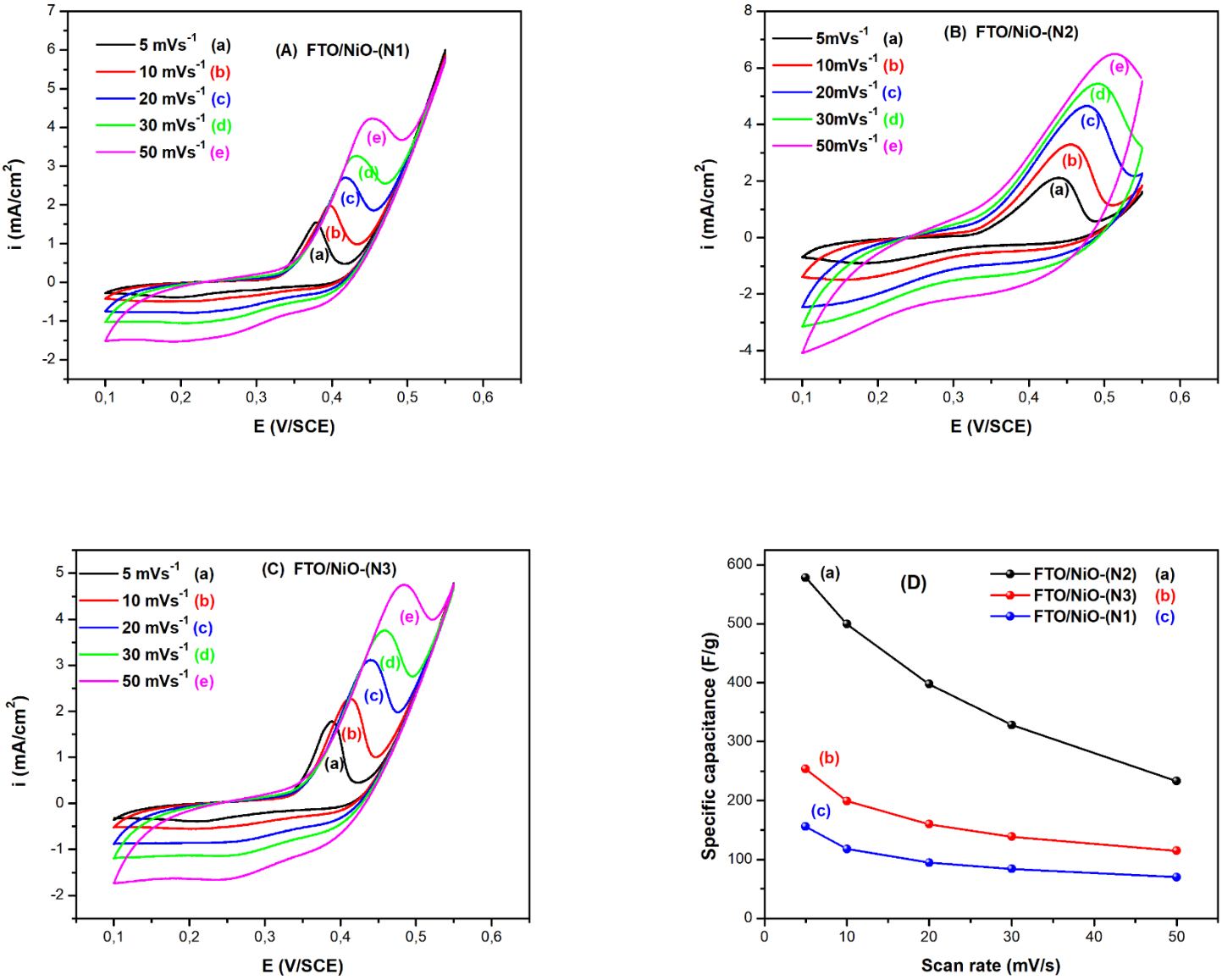

Figure 5. (A-C) Nickel oxide voltammograms at different scan rates in 1M KOH electrolyte, and (D) specific capacitances of the samples at different scan rates.

The specific capacitance in Figure 5c is calculated on the basis of the following equation (7):

$$CS = \frac{\int_{E_1}^{E_2} i(E)\, dE}{2\,(E_1 - E_2)\,mv} \qquad (7)$$

In which SC is the specific capacitance, E_2-E_1 is the potential in cyclic voltammetry window, $\int_{E_1}^{E_2} i(E)dE$ is the voltammetric charge obtained by integration of the CV curve, m is the weight of deposited materiel on the working electrode and ν is the scan rate.

Electrochemical impedance spectroscopy (EIS) was carried out at different applied potentials in the 100 KHz to 50 mHz frequency range. Figure 6 presents the impedance spectra of the NiO samples in KOH electrolyte. Spectra consist in one semicircle at high frequency followed by a straight line at low frequency. The solution resistance R_s and charge transfer resistance R_{ct} can be obtained from the Nyquist plot, Electrochemical impedance spectra demonstrate that PE-mode NiO films present a much-enhanced conductivity than DC-synthesised ones.

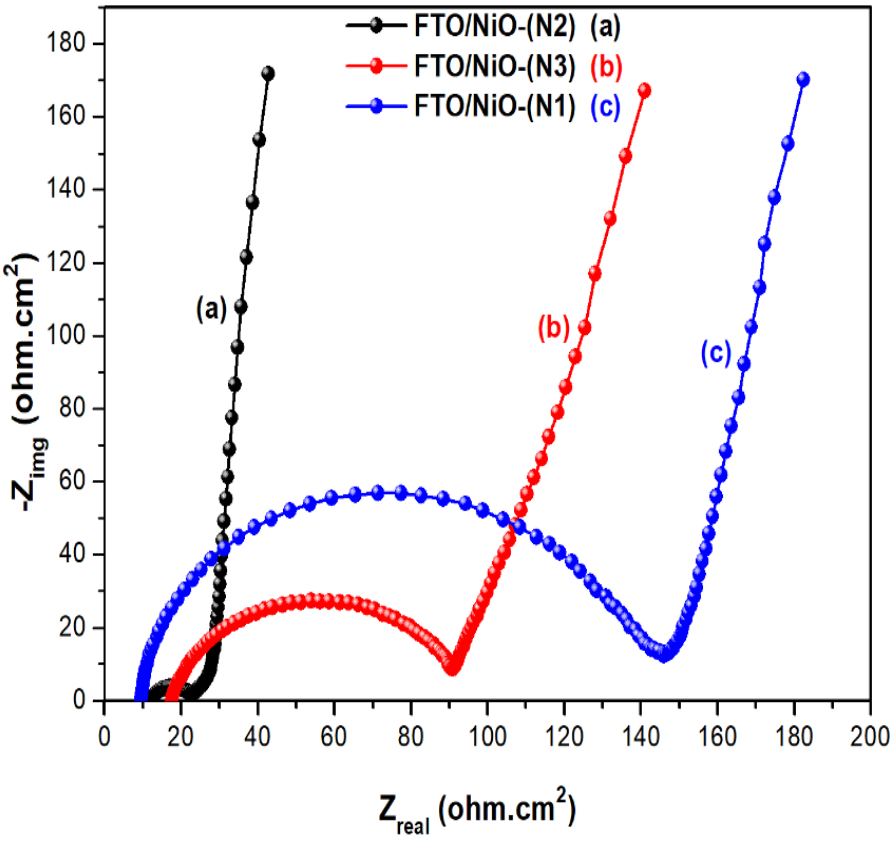

Figure 6. Nyquist plots of FTO/NiO (a)-(N2), (b)-(N3) and (c)-(N1) in 1M KOH electrolyte.

The electrode materials were subjected to galvanostatic charge–discharge (GCD) experiments. Figure 7 shows the GCD curves of FTO/NiO films at different current densities of 0.5, 1, 2, 3, and 5 Ag^{-1} with voltages between 0.1 and 0.4 V. Typical charge−discharge curves show that the charge–discharge potential exhibits a linear response with time. This indicates a good reversibility during the charge and discharge processes, thus demonstrating potentially useful capacitive behavior. All electrode materials showed two stages of voltage drop, with a rapid discharge in the initial potential region and a relative delay in the second potential region, signifying superior electrochemical performances. It is also found that with increasing current density, the discharge times of all electrode materials decrease.

FTO/NiO-(N2) nanoparticles achieved the highest discharge time among the materials tested, showing the best specific capacitance as demonstrated with CV and EIS analyses. Specific capacitances at different current densities of the electrode materials were calculated using equation (8).

$$SC = it / m\Delta v \tag{8}$$

where i/m is the current density used, Δv is the potential window, and t is the discharge time in seconds. The FTO/NiO-(N2) nanoparticles achieved the highest specific capacitance of 1000 Fg^{-1} at a current density of 0.5 Ag^{-1}. On the other hand, FTO/NiO-(N3) and FTO/NiO-(N1) attained specific capacitance values of 350 and 230 F/g at the same current density, respectively. The specific capacitance plot at different current densities is shown in Figure 7. It is seen that with increasing current density, the specific capacitances of all electrode materials decreased. Fewer electrolyte ions can indeed contact the inner electrode space for energy storage at high current density.

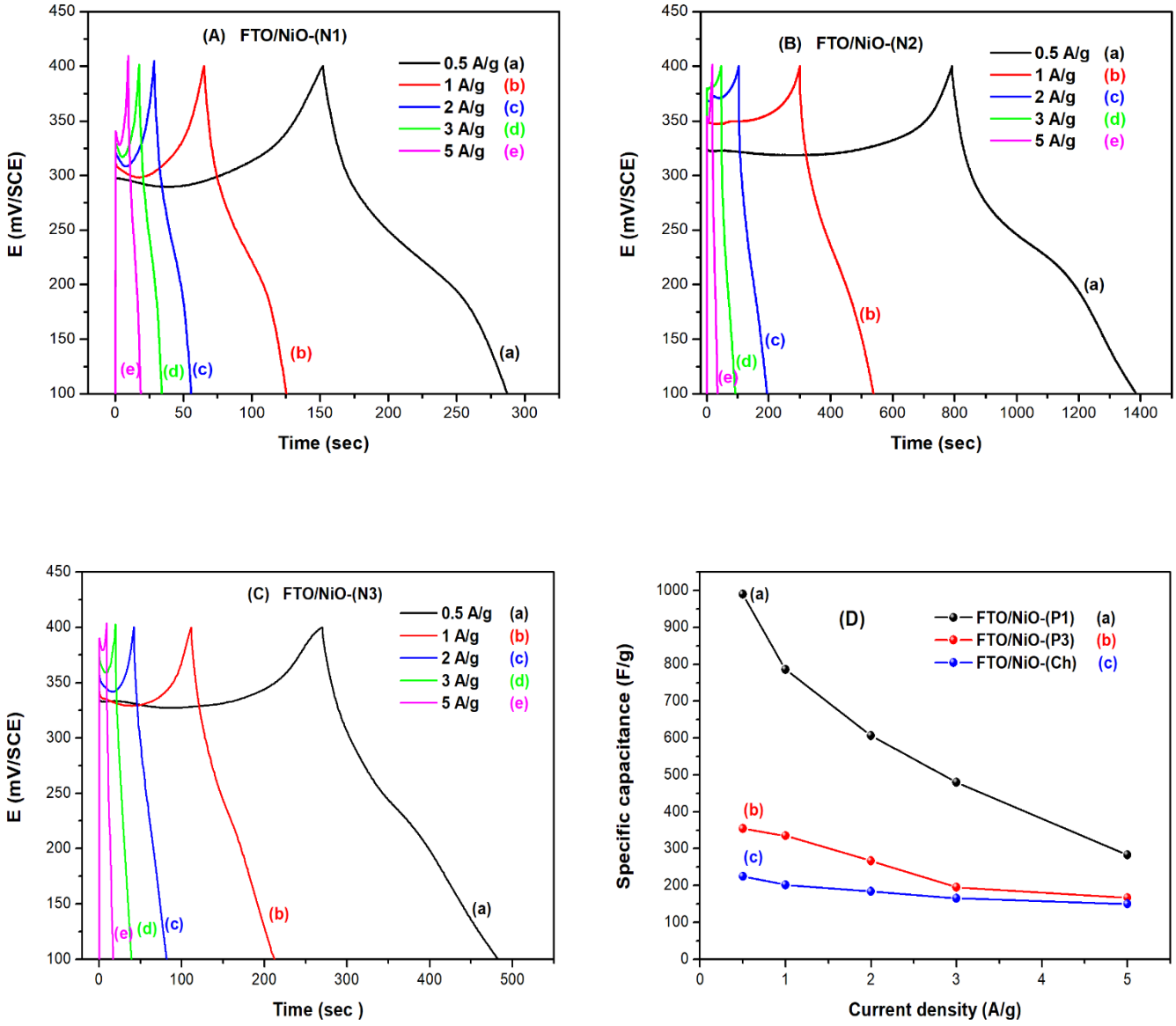

Figure 7. (A-C) discharging time versus current density in 1M KOH electrolyte, (D) specific capacitance variation of the samples as a function of current density.

The GCD cycling performance of the fabricated electrode was monitored in 1 M KOH electrolyte. The NiO electrode was cycled 800 times at 5 Ag^{-1}. SC values of the GCD cycle were calculated using Eq (8). The capacity retention during cycling at the applied current load was obtained from subtraction of the continuous cycle SC values. Figure 8 displays the capacity retention curves of the NiO electrodes during 800 cycles

at constant current load of 5 Ag^{-1}. The GCD cycling performance of the NiO electrode under the applied current load are as follows: SC reduces from 285 $Fg^{-1}$to 255 Fg^{-1} after 800 cycling at 5 Ag^{-1}, which is equivalent to a capacity retention of 90.1% for the FTO/NiO-N1 electrode. This confirms that the prepared porous NiO has a large cycle lifetime and therefore may be a proper material for long-term capacitive applications.

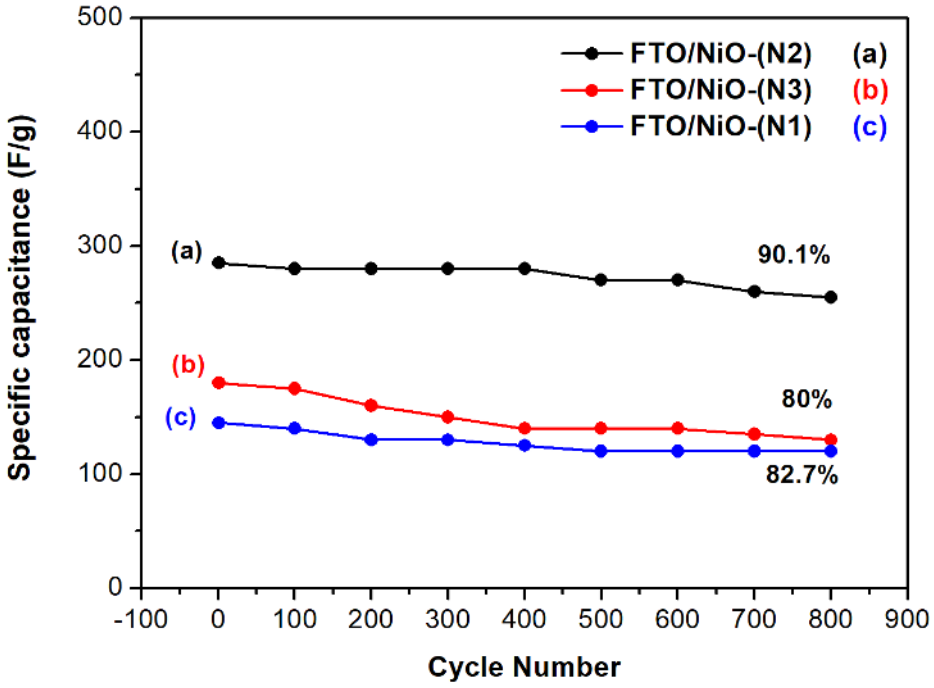

Figure 8: Charge–discharge curves of the fabricated NiO electrodes at the applied current load 5 Ag^{-1} in 1 M KOH electrolyte.

The energy (E) and power density (P) of the fabricated NiO electrodes were also calculated using Eqs. (9) and (10):

$$E = ½CV \tag{9}$$

$$P = E/t \tag{10}$$

The fabricated electrodes are capable of delivering significant energies (E) and power densities (P) at 0.5 Ag^{-1} as illustrated in Table 2. Data confirm the high-performance characters of the prepared porous NiO structures.

Table 2 Energy and power density of NiO electrodes prepared at 0.5 Ag^{-1}.

Electrode	FTO/NiO-(N1)	FTO/NiO-(N3)	FTO/NiO-(N2)
E ($WhKg^{-1}$)	7.2	11.7	45
P (WKg^{-1})	192	198.67	275.04

4. Conclusion

NiO films were electrosynthesized on FTO electrode by chronoamperometry and pulse potentiometry. Electrochemical preparation parameters affect the oxide morphology and capacitive performance of the film. Larger specific capacitance is obtained for high frequency pulse electrodeposited (PE) NiO than for conventional electrodeposition (DE).

NiO electrode capacitive performance was evaluated by CV and charge–discharge. It shows that electrodes prepared at on-time t_{on} = 1s exhibit SC value of 1000 Fg^{-1} at 0.5 Ag^{-1} current loads, as well as 90.1% capacity retention after 800 GCD cycles at 5 Ag^{-1}. Results demonstrate that the as prepared porous NiO electrode is a promising material for long-term capacitive applications.

Reference

[1] K. Gérardin, S. Raël, C. Bonnet, D. Arora, F. Lapicque, Direct coupling of PEM fuel cell to supercapacitors for higher durability and better energy management, Fuel. Cell. 18 (2018) 315-325. doi: 10.1002/fuce.201700041.

[2] Z. Zi-Bo, H. Ke-Jing, W. Xu, Superior mixed Co-Cd selenide nanorods for high performance alkaline battery-supercapacitor hybrid energy storage, Nano Energy. 47 (2018) 89-95. doi: 10.1016/j.nanoen.2018.02.059.

[3] S. Li, W. Paul, F. Kaiwu, N. Zhang, Multi-objective component sizing for a battery-supercapacitor power supply considering the use of a power converter, Energy. 142 (2018) 436-446. doi: 10.1016/j.energy.2017.10.051

[4] S. Cao, B. Li, R. Zhu, H. Pang, Design and synthesis of covalent organic frameworks towards energy and environment fields, Chemical Engineering Journal. 355 (2019) 602-623. doi: 10.1016/j.cej.2018.08.184

[5] G. Zhang, X. Xiao, B. Li, P. Gu, H. Xue, H. Pang, Transition metal oxides with one-dimensional/one-dimensional-analogue nanostructures for advanced supercapacitors, J. Mater. Chem. A. 5 (2017) 8155. doi: 10.1039/c7ta02454a

[6] Y. Xu, B. Li, S. Zheng, P. Wu, J. Zhan, H. Xue, Q. Xu, H. Pang, Ultrathin two-dimensional cobalt-organic framework nanosheets for high-performance electrocatalytic oxygen evolution, J. Mater. Chem. A. 6 (2018) 22070-22076. doi: 10.1039/C8TA03128B

[7] A. Sayah, F. Habelhames, A. Bahloul, B. Nessark, Y. Bonnassieux, D. Tendelier, M.E. Jouad, Electrochemical synthesis of polyaniline-exfoliated graphene composite films and their capacitance properties, J. Electroanal. Chem. 818 (2018) 26–34. doi: 10.1016/j.jelechem.2018.04.016.

[8] R.J. Deokate, R.S. Kalubarme, P. Chan-Jin, C.D. Lokhande, Simple synthesis of NiCo2O4 thin films using spray pyrolysis for electrochemical supercapacitor application: a novel approach, Electrochim. Acta, 214 (2017) 378-385. doi: 10.1016/j.electacta.2016.12.034.

[9] P. Cao, L. Wang, Y. Xu, Y. Fu, X. Ma, Facile hydrothermal synthesis of mesoporous nickel oxide/reduced graphene oxide composites for high performance electrochemical supercapacitor, Electrochim. Acta. 157 (2015) 359-368. doi: 10.1016/j.electacta.2014.12.107

[10] A. Bahloul, B. Nessark, E. Briot, H. Groult, A. Mauger, K. Zaghib, C.M. Julien, Polypyrrole-covered MnO_2 as electrode material for supercapacitor, J. Power Sources. 240 (2013) 267-272. doi: 10.1016/j.jpowsour.2013.04.013.

[11] P. Geng, Shasha Zheng, H. Tang, R. Zhu, L. Zhang, S. Cao,H. Xue, H. Pang, Transition Metal Sulfides Based on Graphene for Electrochemical Energy Storage, Adv. Energy Mater. 08 (2018) 1703259. doi: 10.1002/aenm.201703259

[12] B. Li, P. Gu, Y. Feng, G. Zhang, K. Huang, H. Xue, H. Pang, Ultrathin Nickel–Cobalt Phosphate 2D Nanosheets for Electrochemical Energy Storage under Aqueous/Solid-State Electrolyte, Advanced Functional Materials. 27 (2017) 1605784. doi: 10.1002/adfm.201605784

[13] S. Zheng, X. Li, B. Yan, Q. Hu, Y. Xu, X. Xiao, H. Xue, H. Pang, Transition-Metal (Fe, Co, Ni) Based Metal-Organic Frameworks for Electrochemical Energy Storage, Adv. Energy Mater. 7 (2017) 1602733. doi: 10.1002/aenm.201602733

[14] P. Simon, Y. Gogotsi, Materials for electrochemical capacitors, Nanoscience and Technology: A Collection of Reviews from Nature Journals. (2009) 320-329. doi: 10.1142/9789814287005_0033.

[15] M. Aghazadeh, M.R. Ganjali, Electrosynthesis of highly porous NiO nanostructure through pulse cathodic electrochemical deposition: heat-treatment (PCED-HT) method

with excellent supercapacitive performance, J. Mater. Sci. -Mater. Electron. 28 (2017) 8144-8154, doi: 10.1007/s10854-017-6521-6.
[16] Y. Li, Y. Xu, W. Yang, W. Shen, H. Xue, H. Pang, MOF-Derived Metal Oxide Composites for Advanced Electrochemical Energy Storage, Small. 14 (2018) 1704435. doi: 10.1002/smll.201704435
[17] J. Lin, H. Jia, H. Liang, S. Chen, Y. Cai, J. Qi, C. Qu, J. Cao, W. Fei, J. Feng, In Situ Synthesis of Vertical Standing Nanosized NiO Encapsulated in Graphene as Electrodes for High-Performance Supercapacitors, Adv. Sci. 5 (2018) 1700687. doi: 10.1002/advs.201700687.
[18] D.P. Dubal, D.S. Dhawale, R.R. Salunkhe, V.S. Jamdade, C.D. Lokhande, Fabrication of copper oxide multilayer nanosheets for supercapacitor application, J. Alloys Compd. 492 (2010) 26-30. doi: 10.1016/j.jallcom.2009.11.149.
[19] S.H. Oh, L.F. Nazar, Direct synthesis of electroactive mesoporous hydrous crystalline RuO_2 templated by a cationic surfactant, J. Mater. Chem. 20 (2010) 3834-3839. doi: 10.1039/B926734D.
[20] X. Lu, G. Wang, T. Zhai, M. Yu, J. Gan, Y. Tong, Y. Li, Hydrogenated TiO2 nanotube arrays for supercapacitors, Nano letters. 12 (2012) 1690-1696. doi: 10.1021/nl300173j.
[21] R. Liu, Z. Jiang, Q. Liu, X. Zhu, L. Liu, L. Nia, C. Shen, Novel red blood cell shaped α-Fe 2 O 3 microstructures and FeO (OH) nanorods as high capacity supercapacitors, RSC Advances. 5 (2015) 91127-91133. doi: 10.1039/C5RA14619D.
[22] Y. Wang, Y. Xia, Electrochemical capacitance characterization of NiO with ordered mesoporous structure synthesized by template SBA-15, Electrochim. Acta. 51 (2006) 3223-3227. doi: 10.1016/j.electacta.2005.09.013.
[23] M. Jing, C. Wang, H. Hou, Z. Wu, Y. Zhu, Y. Yang, X. Jia, Y. Zhang, X. Ji, Ultrafine nickel oxide quantum dots embedded with few-layer exfoliative graphene for an asymmetric supercapacitor: Enhanced capacitances by alternating voltage, J. Power Sources. 298 (2015) 241-248. doi: 10.1016/j.jpowsour.2015.08.039.
[24] S. Koussi-Daouda, O. Majerusa, D. Schamingb, T. Pauporté, Electrodeposition of NiO films and inverse opal organized layers from polar aprotic solvent-based electrolyte, Electrochim. Acta. 219 (2016) 638-646. doi: 10.1016/j.electacta.2016.10.074
[25] K. Nakaoka, J. Ueyama, K. Ogura, Semiconductor and electrochromic properties of electrochemically deposited nickel oxide films, J. Electroanal. Chem. 571 (2004) 93-99. doi: 10.1016/j.jelechem.2004.05.003.
[26] M.S. Wu, C.H. Yang, M.J. Wang, Morphological and structural studies of nanoporous nickel oxide films fabricated by anodic electrochemical deposition techniques, Electrochim. Acta. 54 (2008) 155-161. doi: 10.1016/j.electacta.2008.08.027
[27] L. Zhao, G. Su, W. Liu, L. Cao, J. Wang, Z. Dong, M. Song, Optical and electrochemical properties of Cu-doped NiO films prepared by electrochemical deposition, Appl. Surf. Sci. 257 (2011) 3974-3979. doi: 10.1016/j.apsusc.2010.11.160.
[28] S. Koussi-Daoud, Y. Pellegrin, F. Odobel, B. Viana, T. Pauporté, Electrodeposition of NiO films from various solvent electrolytic solutions for dye sensitized solar cell application, Oxide-based Materials and Devices VIII, International Society for Optics and Photonics. 10105 (2017) 1010526. doi: 10.1117/12.2252251.
[29] Y. Ghalmi, F. Habelhames, A. Sayah, A. Bahloul, B. Nessark, H. Derbal-Habak, Y. Bonnassieux, J.M. Nunzi, Enhancement of the capacitance properties and the photoelectrochemical performances of P3HT film by incorporation of nickel oxide nanoparticles, *Ionics*. (2018). doi: 10.1007/s11581-018-2781-2
[30] S.D. Peacor, T. Hibma, Reflection high-energy electron diffraction study of the growth of NiO and CoO thin films by molecular beam epitaxy, Surf. Sci. 301 (1994) 11-18. doi: 10.1016/0039-6028(94)91283-1.

[31] J.X. Shen, M.T. Kief, Exchange coupling between NiO and NiFe thin films, J. Appl. Phys. 79 (1996) 5008-5010. doi: 10.1063/1.361556.
[32] Y. Wang, Q.Z. Qin, A nanocrystalline NiO thin-film electrode prepared by pulsed laser ablation for Li-ion batteries, J. Electrochem. Soc. 149 (2002) A873-A878. doi: 10.1149/1.1481715.
[33] E. Fujii, A. Tomozawa, H. Torii, R. Takayama, Preferred orientations of NiO films prepared by plasma-enhanced metalorganic chemical vapor deposition, Jpn. J. Appl. Phys. 35 (1996) L328. Doi: 10.1143/JJAP.35.L328.
[34] M. Lakhdari, F. Habelhames, B. Nessark, M. Girtan, H. Derbal-Habak, Y. Bonnassieux, D. Tondelier, J.M. Nunzi, Effects of pulsed electrodeposition parameters on the properties of Zinc oxide thin-films to improve the photoelectrochemical and photoelectrodegradation efficiency, Eur. Phys. J. Appl. Phys. 84 (2018) 21102. Doi: 10.1051/epjap/2018180227
[35] I.H. Lo, J.Y. Wang, K.Y. Huang, J.H Huang, W.P. Kang, Synthesis of $Ni(OH)_2$ nanoflakes on ZnO nanowires by pulse electrodeposition for high-performance supercapacitors, J. Power. Sources. 308 (2016) 29-36. Doi: 10.1016/j.jpowsour.2016.01.041
[36] M.S. Wu, Y.A. Huang, C.H. Yang, J.J. Jow, Electrodeposition of nanoporous nickel oxide film for electrochemical capacitors, Int. J. Hydrogen Energy. 32 (2007) 4153-4159. doi: 10.1016/j.ijhydene.2007.06.001.
[37] A.C. Sonavanea, A.I. Inamdarab, P.S. Shindea, H.P. Deshmukhc, R.S. Patila, P.S. Patil, Efficient electrochromic nickel oxide thin films by electrodeposition, J. Alloys Compd. 489 (2010) 667-673. doi: 10.1016/j.jallcom.2009.09.146.
[38] S. Z. F. Rodzi, Y. Mohd, Electrochromic Performance of NiO Films in Alkaline Medium, Advanced Materials Research. 748 (2013) 51-55. doi: 10.4028/www.scientific.net/AMR.748.51.
[39] M. Wu, C. Yang, Electrochromic properties of intercrossing nickel oxide nanoflakes synthesized by electrochemically anodic deposition, Appl. Phys. Lett. 91 (2007) 33109–1. doi: 10.1063/1.2759270.
[40] M. Wu, Y. Huang, J. Jow, W. Yang, C. Hsieh, H. Tsai, Anodically potentiostatic deposition of flaky nickel oxide nanostructures and their electrochemical performances, Int. J. Hydrogen Energy. 33 (2008) 2921–2926. doi: 10.1016/j.ijhydene.2008.04.012.
[41] L.A. Saghatforoush, M. Hasanzadeh, S. Sanati, R. Mehdizadeh, $Ni(OH)_2$ and NiO Nanostructures: Synthesis, Characterization and Electrochemical Performance, Bull. Korean Chem. Soc. 33 (2012) 2613. doi: 10.5012/bkcs.2012.33.8.2613
[42] M.A. Gondal, T.A. Saleh, Q.A. Drmosh, Synthesis of nickel oxide nanoparticles using pulsed laser ablation in liquids and their optical characterization, Applied Surface Science 258 (2012) 6982. doi: 10.1016/j.apsusc.2012.03.147
[43] H.M. Shiri, M. Aghazadeh, Synthesis, Characterization and Electrochemical Properties of Capsule-Like NiO Nanoparticles, J. Electrochem. Soc. 159 (2012) E132-E138. doi: 10.1149/2.106206jes
[44] A. Rahdar, M. Aliahmad, Y. Azizi, NiO Nanoparticles: Synthesis and Characterization, JNS 5 (2015) 145- 151. doi: 10.7508/JNS.2015.02.009
[45] M. Mondal, B. Das, P. Howli, N.S. Das, K.K. Chattopadhyay, Porosity-tuned NiO nanoflakes: Effect of calcination temperature for high performing supercapacitor application, J. Electroanal. Chem. 813 (2018) 116-126. doi: 10.1016/j.jelechem.2018.01.049.